ISSN 0915-633X

NATIONAL INSTITUTE FOR FUSION SCIENCE

Development of Diagnostic Beams for Alpha Particle Measurement on ITER

M. Sasao, A. Taniike, I. Nomura, M. Wada,
H. Yamaoka and M. Sato

(Received - July 20, 1995)

NIFS-370 Aug. 1995

RESEARCH REPORT
NIFS Series

NAGOYA, JAPAN

Development of Diagnostic Beams for Alpha Particle Measurement on ITER

M. Sasao, A. Taniike, I. Nomura,
M.Wada*, H.Yamaoka**, M.Sato***

National Institute for Fusion Science, Chikusa Nagoya-464-10, Japan
*Department of Electronics, Doshisha Univ. , Tanabe, Kyoto-610-03, Japan
**RIKEN, Wako-351-01, Japan
***Himeji technical Univ., Himeji-671-22, Japan

Abstract

The feasibility of alpha particle measurement using a high energy diagnostic beam in combination with a neutral particle analyzer is examined for a burning plasma on ITER. In order to measure them in the energy range of 0.5 - 3.5 MeV, the required beam energy is around 1 MeV for a $^3He^0$ beam and 3 MeV for a $^6Li^0$ beam with the beam current density of around 1 mA/cm^2 for both cases. Among the various methods to produce such a high energy neutral beam, the acceleration of negative ions is most favorable. Recent results of relatively small-scale experiments on these negative ion sources show that the required current density is now realistic. Some technical problems how to scale-up the ion sources to be used on an ITER-size experiment are also studied on these experiments..

Key Words

alpha particle, diagnostic beam, neutral particle analyzer, ITER, He^0 beam, Li^0 beam, He^- ion source, Li^- ion source

1. Introduction

The velocity distribution of alpha particles in a plasma has been thought to be one of the key items on a burning experiment. Several proposals have been made to measure it. One of them is an alpha particle measurement by using the single or double charge exchange process[1,2,3]. In the first method, the alpha particle captures one electron into an excited state from an atomic particle of a diagnostic beam, or from an ionizing particle in the ablation cloud around a pellet. The velocity distribution of the alpha particles can then be obtained from the Doppler spectrum of the emitted line. In the second method, an alpha particle is neutralized through a two-electron transfer process as

$$^{4}\mathrm{He}^{++} + \mathrm{A}^{q} \text{ -------> } {}^{4}\mathrm{He}^{0} + \mathrm{A}^{q+2} \qquad (1)$$

where $^{4}\mathrm{He}^{0}$ escapes from a plasma, and is detected by an energy analyzer. Here A^{q} represents a beam particle, or an ionizing particle around a pellet, which should be a helium or heavier atom. These methods have been tried in the DT experiments of TFTR using the ablation cloud from lithium pellets, and lots of interesting results are obtained[4].

In this paper, a measurement system applicable to the ITER project is examined using a high-energy neutral beam in combination with a neutral-particle analyzer. The donor atom density of the beam is usually much less than that from a pellet, but the measurement can be performed continuously without disturbing the bulk plasma. As has been pointed out in the earlier works [1,2], beam energy in the range of that of the alpha particles is preferable. The escaped neutral particles should be detected at a forward angle, in order to make the relative velocity between the donor atom and the alpha particle small enough. It is considered that the relevant charge exchange cross section (1) decreases rapidly when the relative energy is greater than 200 keV. In the present work, only helium and lithium beams are considered, since a heavier particle beam requires a higher acceleration voltage to achieve the same beam velocity.

The beam attenuation has been thought to be extremely serious for such a large experimental device as ITER, especially when the plasma density is high. Based on a possible experimental configuration of the ITER, the beam attenuation in the plasma and expected signal levels at the detector are estimated in the next section. Requirements of the beam energy and current are also examined. In Section 3, various methods to produce such beams are then discussed, and the activities on the development of negative ion sources for this purpose, and recent results of relatively small-scale experiments are reviewed. Summarizing the present feasibility studies, the scope to scale-up the ion sources to be used in ITER-sized experiments is examined in Section 4.

2 Scheme of Measurement

2.1 Beam Attenuation

In the present design of the ITER, it is not possible to inject a beam vertically if neutralized particles are to be detected at a forward angle. The bottom of the vacuum vessel is fully occupied by the divertor components. Figure. 1 schematically illustrates the possible geometry of the tangential injection of a probing beam. Alpha particles, which are neutralized in the beam and pass through the port adjacent to the beam dump, are detected at the biological shield. With this configuration, the detector covers the entire region of the radial position in the plasma, from r=0 to r=a. The plasma lengths for the incoming beam, that for outgoing $^4He^0$ particles, and viewing angles of the detector are listed in Table 1. The values are given for two cases, when the observation volume is located at r=0 (**A**), and at r=0.9a (**B**).

The attenuation of the beam in the plasma of $T_e(r)$= 10 keV x $\{1-(r/a)^2\}^2$ is evaluated, including electron impact ionization, ion impact ionization and charge exchange processes. Here, contamination by impurity ions of 0.3% O^{8+} and 0.03% Fe^{26+} are assumed. The ionization cross section by naked impurity ions $\sigma_i^{imp}(v)$ is assumed to be proportional to that by protons of the same velocity, and given by

$$\sigma_i^{imp}(v) = z^2 \sigma_i^{p}(v).$$

In Fig.2, beam fractions that penetrate into the central position **A**(Fig.1) are shown as a function of the central plasma density, for (a)neutral beams of He^0, and (b)that of Li^0. The beams are injected with velocities of v_α, 0.8 v_α, 0.6 v_α, and 0.4 v_α. Here, v_α is the virgin alpha particle velocity. The main contribution to beam attenuation results from ionization processes associated with impact by plasma ions and impurity ions. The penetration of a beam greatly depends on the beam velocity and plasma density. More than several % of the He^0 beam particles may survive at the center when the beam velocity is greater than 0.6 v_α ($E_b \geqq 1$ MeV for a $^3He^0$ beam), and the plasma density less than 2 x $10^{20}/m^3$. On the other hand, tolerable penetration of a Li^0 beam occurs only when the beam velocity is greater than 0.8 v_α ($E_b \geqq 3.4$ MeV for the $^6Li^0$ beam) and the plasma density less than $10^{20}/m^3$.

2.2 Expected counting rates

The number of neutralized alpha particles per unit velocity bin, C(v) dv, detected at the analyzer viewing the plasma volume of ΔV with the solid angle of $d\Omega$, can be estimated using the following equation,

$$C(v)\,dv = \eta(v) \bullet n_{\alpha}\,(v,r)\; n_B\,(r) \bullet \sigma_{20}\, v_{rel} \bullet \Delta V \bullet d\Omega \bullet dv\,.$$

Here, n_{α} (v,r) and n_B (r) are the local densities of alpha particles and beam particles, respectively, σ_{20} is the two-electron capture cross section, and v_{rel} the relative velocity between an alpha particle and an injected neutral atom. The transmission coefficient of outgoing particles $\eta(v)$ is estimated in the same manner as in Section 2.1, and is included in the above equation.

The counting rates expected for a neutral beam injection of the "100-mA" port-through atom current (1 mA/cm^2, 10 cm x 10 cm) are estimated for an ITER plasma of $n_e(0) = 10^{20}/m^3$ The plasma has a 1% alpha particle density of a classical slowing-down velocity distribution. The attenuation's of the injected beam and neutralized particles are considered. The expected spectra of two $^3He^0$ beam injections (a) and (b), and of a $^6Li^0$ beam(c). are shown in Fig. 3. Here the observation volumes are located in the central area for (a) and (c) and in the edge area for (b). The acceptance area of the analyzer is assumed to be 1 cm^2 for each channel covering the velocity of 1/10 v_{α}.

Using a $^3He^0$ beam of $0.8\ v_{\alpha} \geq v_B \geq 0.6\ v_{\alpha}$, counting rates per channel exceed 0.5 x 10^4 /s in the spectrum region of $0.4v_{\alpha} \leq v \leq 0.9\ v_{\alpha}$, ($0.5\ MeV \leq E \leq 2.8MeV$) for the geometry that views most of the entire region of the plasma radius. For the $^6Li^0$ beam, nearly the same counting rates can be expected when the outer region is viewed, and those from the central region are about one order less, as shown in Fig.3c, where $v_B \geq 0.8\ v_{\alpha}$ and $n_e(0) = 10^{20}/m^3$

The background noise of the detector could greatly depend on the neutron flux, gamma-ray flux, and their associate energy spectra. The (n,p) and (n, α) nuclear reactions are usually the origin the background pulse spectrum in the alpha particle energy region of the present interest. Their cross sections are generally on the order of 1mb. The flux rate of neutrons in the energy region above the proton or the alpha production threshold, namely $E_n \geq 3$MeV, would be about 10^7-10^{10}/cm^2/sec in the area of the biological shield. Assuming the thickness of the particle detector of 10^{21}/cm^2, the background pulse rate would be in the range of 10-10^4/cm^2/sec .

The estimated counting rate using an 0.1A-$^3He^0$ beam (1mA/ cm^2, 100 cm^2) should be above the background noise level, and that with an 0.1A-$^6Li^0$ beam should also be tolerable if the background level is reduced by use of a beam modulation technique, or an additional neutron shield.

3 Diagnostic beams of $^3He^0$ and $^6Li^0$

In order to produce a $^3He^0$ or a $^6Li^0$ beam in the energy region above 1 MeV, the conventional method of electron attachment to positive ions in a gas becomes very inefficient. From detailed calculations of charge fractions and the fraction of long-life metastable states in a gas cell, starting with various positive ions and negative ions of helium [5], the production of a ground state beam of He^0 from He^- is most efficient for energies greater than 0.4 MeV. The typical efficiency is about 15 % at E = 1-2 MeV.

The neutralization efficiency of Li^+ into Li^0 is also presumed to be less than 1% at energies greater than 1 MeV, while that of Li^- is 50%. Therefore, the developments of high intensity negative ion sources of He^- and Li^- are essential to realize this measurement scheme.

In order to produce negative ions, three methods are generally used. Some negative ions can be directly extracted from a plasma under a special conditions. More than 50 mA/cm^2 of H$^-$ current has been extracted from a hydrogen plasma in a multicusp source using a magnetic filter[6]. Both Li$^-$ and Na$^-$ have also been directly extracted from their associated plasmas[7-9]. The other two methods are surface production, that by production from a low-work-function surface bombarded by beam particles or plasma ions[10], and production through two-step charge exchange processes[11,12].

3.1 Development of He$^-$ ion sources.

Among the various elements, the production of He$^-$, however, is known to be extremely difficult. The ground state of helium does not form a negative ion, but the a long-life metastable state of 1s2s (^3S) has a small electron affinity of 0.078 eV and a negative ion state of 1s2s2p ($^4P_{5/2}$, $^4P_{3/2}$) can be formed. This is an autodetatchment state having life-times of 10 μs (50%) and 300 μs(50%) .

After much effort to certify the surface production of He$^-$, It has been concluded that the production rate of He$^-$ from a Cs-Mo surface of minimum work function is nearly zero or much less than that of H$^-$ [13]. Moreover, it is known that He$^-$ can not be directly extracted from a helium plasma in a multicusp ion source.

On the other hand, He$^-$ has been produced via a two step process in an alkali metal gas cell, such as Li, Na, Mg, K, Rb, or Cs [14, 15]. The maximum value of the He$^-$ fraction of 1.7% is obtained through collisions with a Rb target, at an He$^+$ ion incident energy of 6-9 keV[15]. Using a sodium gas cell, Dimov et al. have reported the production of a 10-mA He^- beam at 12 keV in a 100 μsec pulse with a current density of 2.6 mA/cm^2 [11]. A 70-mA He^- beam was also generated in a pulsed mode by Hooper et al.[12].

Development of an He^- source using a Rb gas cell in a DC operation has been recently initiated for the purpose of application to the alpha-particle measurement[16]. The essential point of the development can be found that of an effective and long-life Rb gas cell, which can be operated in a DC, or a modulated mode. In the present preliminary experiments, the Rb cell was operated in a DC mode at high pressure to convert He^+ to He^- at an efficiency of greater than 2 %. Since a positive ion current density of greater than 200mA/cm^2 can be expected using a conventional source, a negative current density of 4mA/cm^2 should be feasible.

3.2 Development of Li^- ion sources.

Lithium negative ions can be produced using the three methods mentioned above, that is, by the volume production in a plasma[7,8], surface production[17], and charge-exchange process[18]. There are some difficulties, however, in the practical use of an ion source to generate a beam. These difficulties include a lithium drain and lithium adherence to electrodes during a long operation, and impurity contamination in the extracted beam.

Walther, Leung and Kunkel had directly extracted Li^- ions from a lithium plasma confined in a small multicusp ion source, having a current density of 1.9 mA/cm^2[7]. Similar to H^- volume production, it is thought that Li_2 molecules play an important role in the negative ion production in a plasma, with higher vapor pressure being favorable for the production of Li_2[8]. In these production experiments, a small lithium block was placed in the ion source with the lifetime of the operation being limited by the consumption of the metal or the adherence of the lithium to the electrodes. The charge exchange method has the same problem. The conversion rate of Li^+ to Li^- is 4% at most. In order to achieve a high current density of positive ions, the consumption and the drain of lithium are inevitable. The surface production method is more efficient in the sense of the amount of consumption. A production of 0.1 mA/cm^2 Li^- ions has been reported, with the help of Cs coverage and oxygen adsorption on the surface[16]. There is, however, a problem in that large amounts of impurity ions, such as of H^-, C^-, O^-, and OH^- were also simultaneously extracted .

4 Discussions and summary

Alpha particles confined in an ITER plasma can be neutralized by a high energy neutral beams of $^3He^0$ or $^6Li^0$ with beam velocities of 0.6-0.8 v_α. The attenuation of the beam can be tolerated if the central plasma density is less than 3 x $10^{20}/m^3$ for the $^3He^0$ beam, and less than $10^{20}/m^3$ for the $^6Li^0$ beam. If the alpha particle density is 1 % of the plasma density and the port-through current density 1 mA/cm^2 with a cross section of 10 cm x 10 cm, the counting rate would then be sufficient to measure the neutral particle spectra with good statistics. The alpha particle spectrum can be obtained by dividing neutral particle counts by the local beam particle density and the two electron transfer cross section, and by making corrections for beam attenuation and detection efficiency.

The absolute value of the alpha particle density in the high energy region can also be obtained if the absolute value of the beam particle density in the plasma is known. The incoming beam current can be monitored to an accuracy of about 10 %. The attenuation of the beam in the plasma is more serious and should be estimated from the values of $n_e(r)$,$T_e(r)$, and $Z_{eff}(r)$. This can be cross-checked by monitoring the current at the beam dump. Another important factor is the two electron transfer cross section. Total cross sections are measured to an accuracy of around 10 %. Fractions of the metastable state atoms in the neutralized particles, which should be totally attenuated in the plasma, are not known and should be measured. Even when taking into account the various uncertainties, such as those of the beam particle density in the plasma, cross sections, and detection efficiency of the system, the alpha density can be obtained to an accuracy of a factor of 2.

The required beam energy is around 1 MeV for the $^3He^0$ beam and 3 MeV for the $^6Li^0$ beam. Considering the neutralization efficiency, the acceleration of negative ions should be adopted. Recent results of relatively small-scale or short pulse experiments with these negative ion sources reveal that the required current of 100 mA, or current density of 1 mA/cm^2 can be attained, and the diagnostic beam will be realized after some technical R & D works.

The authors are much indebted to Professors Iiyoshi, Fujiwara, Fujita, and Kuroda for encouragement in the development of negative ion sources. The authors are also grateful for useful discussions with Professors T.Kato and H. Tawara. This work was carried out under the Collaboration Research Program at the National Institute for Fusion Science, and the Collaboration Research Program of the Graduate Univ. of Advanced Studies.

Table caption

Parameters for two observation position at r=0 (A), and at r=0.9a (B) as shown in Fig. 1

Figure captions

Fig. 1

Schematic illustration of the possible experimental configuration for alpha particle measurement using a diagnostic beam on ITER.

Fig. 2

Beam fractions at position A in Fig. 1, for a neutral beam of He^0 (a), and of Li^0 (b), injected with velocities of v_α , 0.8 v_α , 0.6 v_α , and 0.4 v_α . Here v_α is the virgin alpha particle velocity.

Fig.3

The expected spectra of neutralized alpha particles by a 100-mA $^3He^0$ beam for velocities of v_α , 0.8 v_α , 0.6 v_α , and 0.4 v_α when observed with (a) the geometry shown in A in Fig.1, and (b) that shown in B in Fig. 1. Figure (c) is that for the 100-mA $^6Li^0$ beam for velocities of v_α , 0.8 v_α , 0.6 v_α , and 0.4 v_α when observed with the geometry A in Fig.1.

References

[1] D.E.Post et al., Fusion Technology 1 (1987), 355

[2] M.Sasao et al., Fusion Technology 10 (1986), 236

[3] M.Sasao et al., Nucl. Fusion 27-2 (1987), 355

[4] R.K.Fisher et al., to be published in Phys. Rev. Lett.

[5] A. Taniike et al., to be submitted.

[6] Y.Takeiri et al., to be published in Rev. Sci. Instrum. 66-3 (1995)

[7] S.R.Walther et al., Appl. Phys.Lett. 51 (1987) 566

[8] M.Wada et al., Rev. Sci. Instrum. 61-1 (1990) 433

[9] M.Sasao et al., Rev. Sci. Instrum. B55 (1991) 318
H.Yamaoka et al., Jpn. J. Appl. Phys. 32 (1993) 3659

[10] M.Wada et al., J. Appl. Phys. 67 (1990) 6334

[11] G.I. Dimov and G.V.Roslyakov, Pribory i Tikhnika Eksperimenta, No. 3, (1974), 31

[12] E.B.Hooper et al., Rev. Sci. Instrum. 51-8 (1980) 1067

[13] M.Sasao et at, Rev. Sci. Instrum. 61-1 (1990) 418

[14] A.S. Schlachter et at, Phy. Rev. 174 (1968) 201
H.B.Gilbody et at, J. Phys. B 2, (1969) 465
R.A.Baragiola et at, Nucl. Instrum. Methods, 110 (1973) 507

[15] R.J. Girnius et at, Nucl. Instrum. Methods, 137 (1976) 373

[16] M.Sasao et al., to be published in Ann. Rep. Nat. Ins. Fusion Sci. 1994/1995

[17] M.Wada et at, Nucl. Instrum. Methods, B37/38 (1989) 132

[18] E. Steffens, IEEEE Trans. Nucl. Sci. NS-23 (1976) 1145

Table 1
Parameters for two observation position at r=0 (A), and at r=0.9a (B) as shown in Fig. 1

position	r	observation angle from the beam direction	pass length of incoming beam (m)	plasma thickness of incoming beam (m^{-2})*	pass length of outgoing beam (m)	plasma thickness of outgoing beam (m^{-2})*	lenth to the detector (m)
A	0.	17^o	7.3	$5.7 \times n_e(0)$	5.3	$3.82 \times n_e(0)$	13
B	0.9 a	11^o	0.42	$0.04 \times n_e(0)$	10.8	$6.26 \times n_e(0)$	20

*assumig $n_e(r) = n_e(0) \{1-(r/a)^2\}$

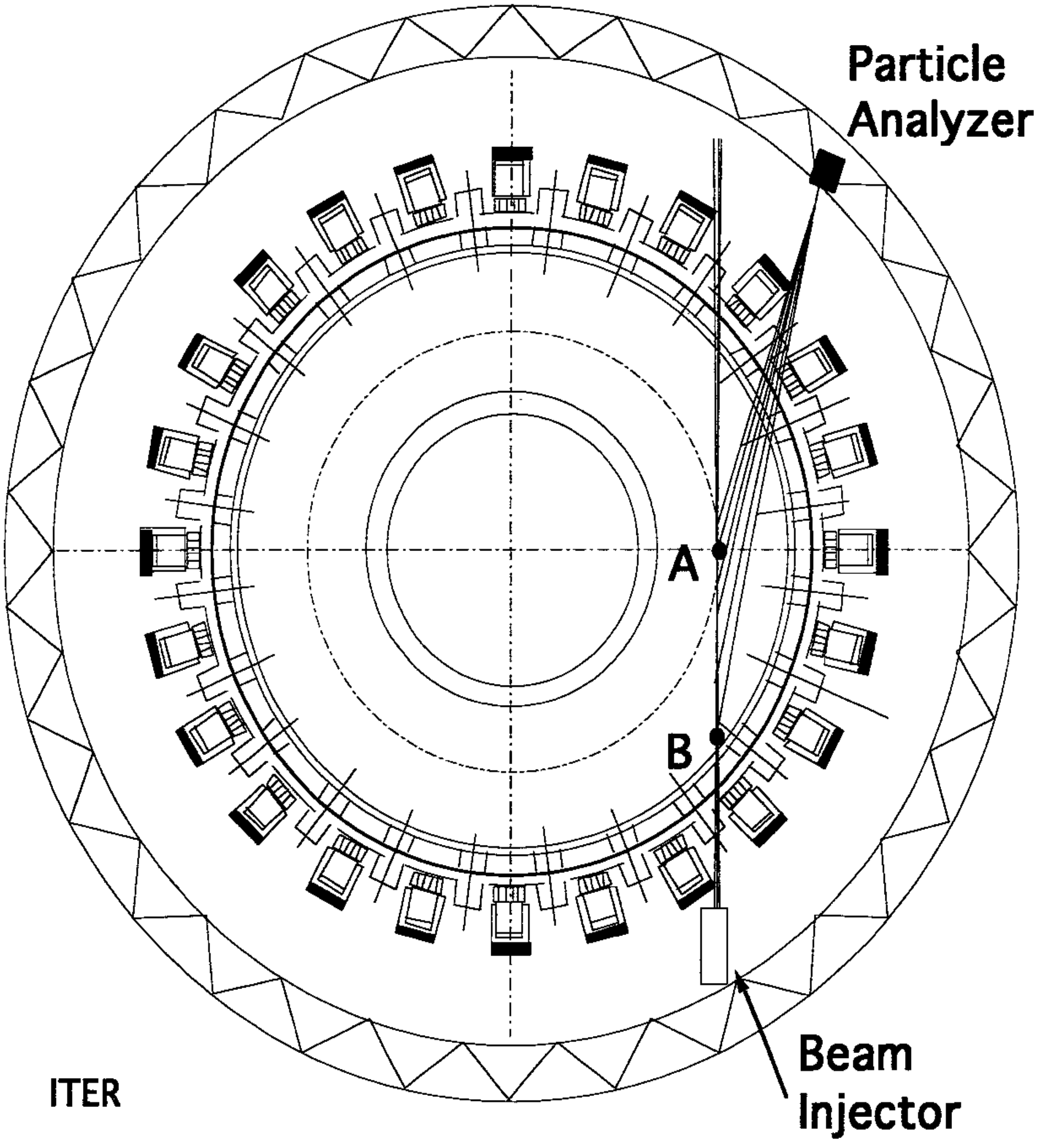

Fig. 1

Schematic illustration of the possible experimental configuration for alpha particle measurement using a diagnostic beam on ITER.

(a) He^0 beam attenuation at point "A"

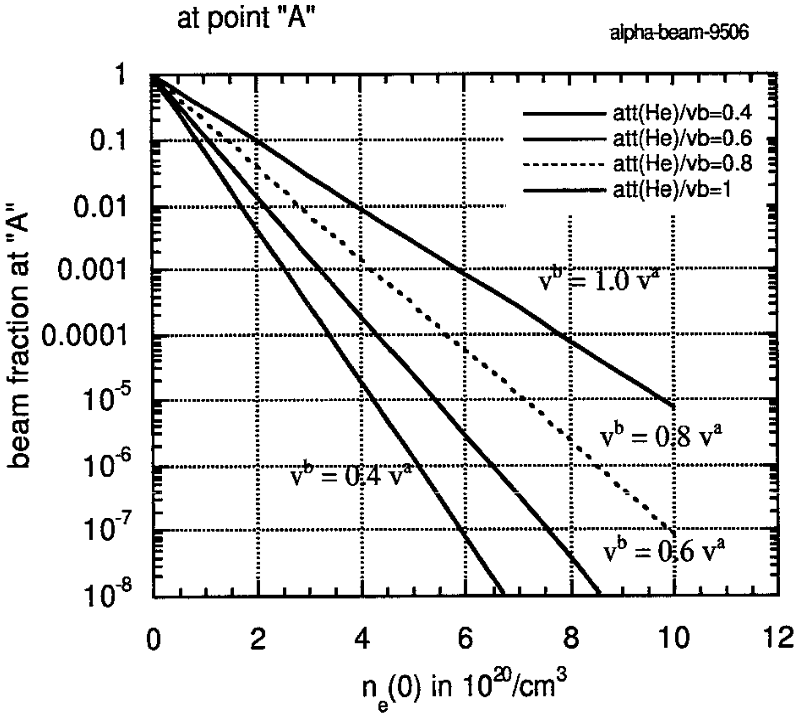

(b) Li^0 beam attenuation at point "A"

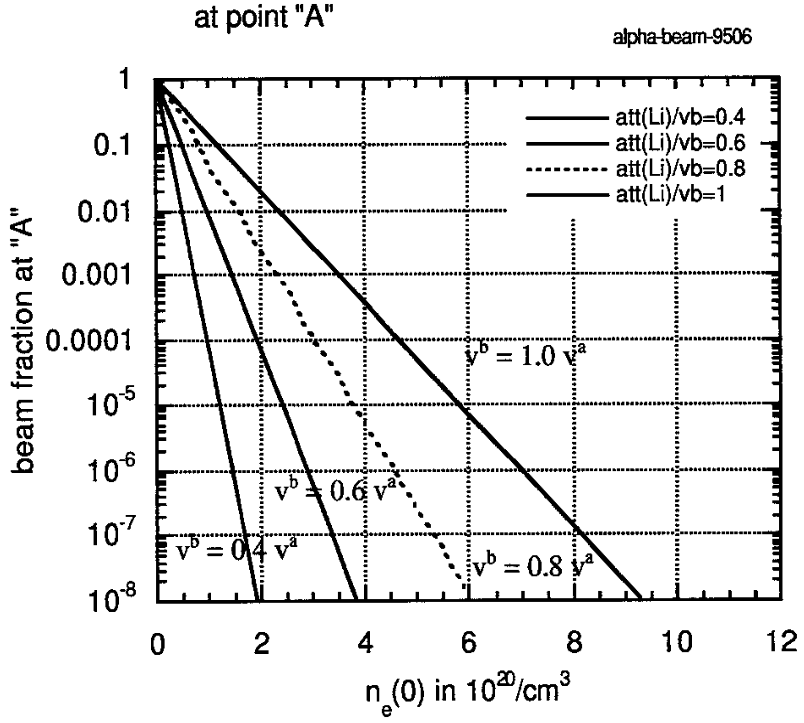

Fig. 2

Beam fractions at position A in Fig. 1, for a neutral beam of He^0 (a), and of Li^0 (b), injected with velocities of v_α, 0.8 v_αa, 0.6 v_α, and 0.4 v_α. Here v_α is the virgin alpha particle velocity.

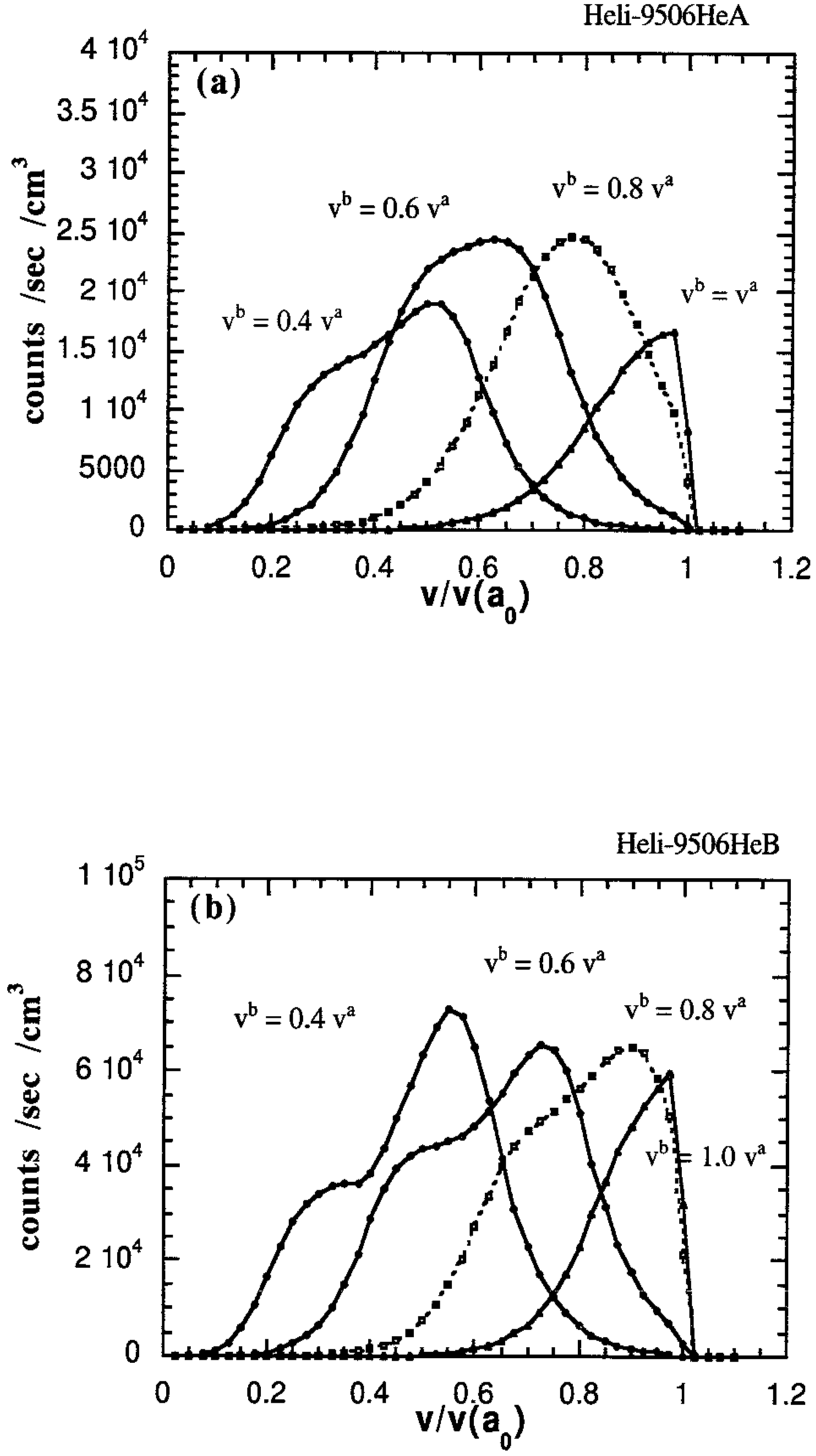
Heli-9506HeA
(a)
counts /sec /cm^3
4 10^4
3.5 10^4
3 10^4
2.5 10^4
2 10^4
1.5 10^4
1 10^4
5000
0
$v^b = 0.6\ v^a$
$v^b = 0.8\ v^a$
$v^b = 0.4\ v^a$
$v^b = v^a$
0
0.2
0.4
0.6
0.8
1
1.2
v/v(a$_0$)
Heli-9506HeB
(b)
counts /sec /cm^3
1 10^5
8 10^4
6 10^4
4 10^4
2 10^4
0
$v^b = 0.6\ v^a$
$v^b = 0.4\ v^a$
$v^b = 0.8\ v^a$
$v^b = 1.0\ v^a$
0
0.2
0.4
0.6
0.8
1
1.2
v/v(a$_0$)

Fig. 3

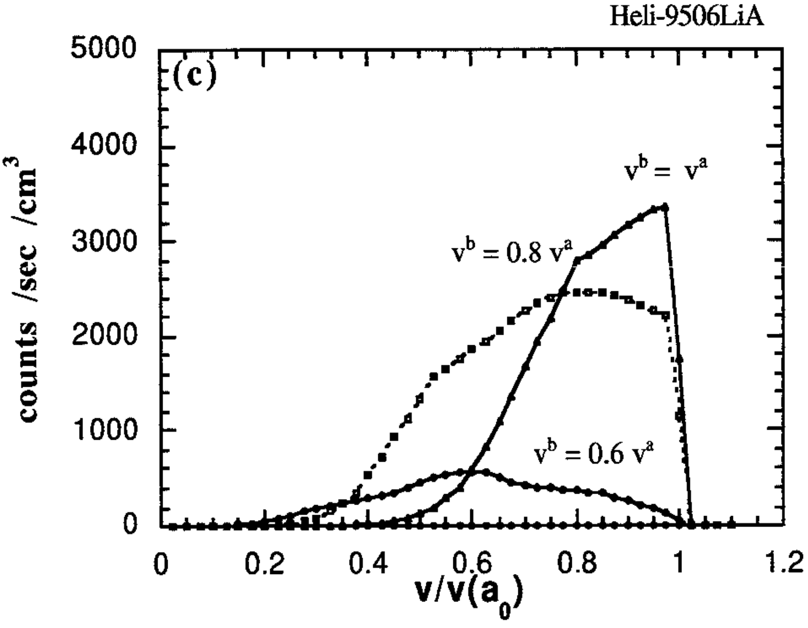

Fig.3

The expected spectra of neutralized alpha particles by a 100-mA ^{3}He^0 beam for velocities of v_α , 0.8 v_α , 0.6 v_α , and 0.4 v_α when observed with (a) the geometry shown in A in Fig.1, and (b) that shown in B in Fig. 1. Figure (c) is that for the 100-mA ^{6}Li^0 beam for velocities of v_α , 0.8 v_α , 0.6 v_α , and 0.4 v_α when observed with the geometry A in Fig.1.

Recent Issues of NIFS Series

NIFS-322 A. Iiyoshi, K. Yamazaki and the LHD Group,
Recent Studies of the Large Helical Device; Nov. 1994

NIFS-323 A. Iiyoshi and K. Yamazaki,
The Next Large Helical Devices; Nov. 1994

NIFS-324 V.D. Pustovitov
Quasisymmetry Equations for Conventional Stellarators; Nov. 1994

NIFS-325 A. Taniike, M. Sasao, Y. Hamada, J. Fujita, M. Wada,
The Energy Broadening Resulting from Electron Stripping Process of a Low Energy Au⁻ Beam; Dec. 1994

NIFS-326 I. Viniar and S. Sudo,
New Pellet Production and Acceleration Technologies for High Speed Pellet Injection System "HIPEL" in Large Helical Device; Dec. 1994

NIFS-327 Y. Hamada, A. Nishizawa, Y. Kawasumi, K. Kawahata, K. Itoh, A. Ejiri, K. Toi, K. Narihara, K. Sato, T. Seki, H. Iguchi, A. Fujisawa, K. Adachi, S. Hidekuma, S. Hirokura, K. Ida, M. Kojima, J. Koong, R. Kumazawa, H. Kuramoto, R. Liang, T. Minami, H. Sakakita, M. Sasao, K.N. Sato, T. Tsuzuki, J. Xu, I. Yamada, T. Watari,
Fast Potential Change in Sawteeth in JIPP T-IIU Tokamak Plasmas; Dec. 1994

NIFS-328 V.D. Pustovitov,
Effect of Satellite Helical Harmonics on the Stellarator Configuration; Dec. 1994

NIFS-329 K. Itoh, S-I. Itoh and A. Fukuyama,
A Model of Sawtooth Based on the Transport Catastrophe; Dec. 1994

NIFS-330 K. Nagasaki, A. Ejiri,
Launching Conditions for Electron Cyclotron Heating in a Sheared Magnetic Field; Jan. 1995

NIFS-331 T.H. Watanabe, Y. Todo, R. Horiuchi, K. Watanabe, T. Sato,
An Advanced Electrostatic Particle Simulation Algorithm for Implicit Time Integration; Jan. 1995

NIFS-332 N. Bekki and T. Karakisawa,
Bifurcations from Periodic Solution in a Simplified Model of Two-dimensional Magnetoconvection; Jan. 1995

NIFS-333 K. Itoh, S.-I. Itoh, M. Yagi, A. Fukuyama,
Theory of Anomalous Transport in Reverse Field Pinch; Jan. 1995

NIFS-334 K. Nagasaki, A. Isayama and A. Ejiri
Application of Grating Polarizer to 106.4GHz ECH System on Heliotron-E; Jan. 1995

NIFS-335 H. Takamaru, T. Sato, R. Horiuchi, K. Watanabe and Complexity Simulation Group,
A Self-Consistent Open Boundary Model for Particle Simulation in Plasmas; Feb. 1995

NIFS-336 B.B. Kadomtsev,
Quantum Telegragh : is it possible?; Feb. 1995

NIFS-337 B.B.Kadomtsev,
Ball Lightning as Self-Organization Phenomenon; Feb. 1995

NIFS-338 Y. Takeiri, A. Ando, O. Kaneko, Y. Oka, K. Tsumori, R. Akiyama, E. Asano, T. Kawamoto, M. Tanaka and T. Kuroda,
High-Energy Acceleration of an Intense Negative Ion Beam; Feb. 1995

NIFS-339 K. Toi, T. Morisaki, S. Sakakibara, S. Ohdachi, T.Minami, S. Morita, H. Yamada, K. Tanaka, K. Ida, S. Okamura, A. Ejiri, H. Iguchi, K. Nishimura, K. Matsuoka, A. Ando, J. Xu, I. Yamada, K. Narihara, R. Akiyama, H. Idei, S. Kubo, T. Ozaki, C. Takahashi, K. Tsumori,
H-Mode Study in CHS; Feb. 1995

NIFS-340 T. Okada and H. Tazawa,
Filamentation Instability in a Light Ion Beam-plasma System with External Magnetic Field; Feb. 1995

NIFS-341 T. Watanbe, G. Gnudi,
A New Algorithm for Differential-Algebraic Equations Based on HIDM; Feb. 13, 1995

NIFS-342 Y. Nejoh,
New Stationary Solutions of the Nonlinear Drift Wave Equation; Feb. 1995

NIFS-343 A. Ejiri, S. Sakakibara and K. Kawahata,
Signal Based Mixing Analysis for the Magnetohydrodynamic Mode Reconstruction from Homodyne Microwave Reflectometry; Mar.. 1995

NIFS-344 B.B.Kadomtsev, K. Itoh, S.-I. Itoh
Fast Change in Core Transport after L-H Transition; Mar. 1995

NIFS-345 W.X. Wang, M. Okamoto, N. Nakajima and S. Murakami,
An Accurate Nonlinear Monte Carlo Collision Operator; Mar. 1995

NIFS-346 S. Sasaki, S. Takamura, S. Masuzaki, S. Watanabe, T. Kato, K. Kadota,
Helium I Line Intensity Ratios in a Plasma for the Diagnostics of Fusion

Edge Plasmas; Mar. 1995

NIFS-347 M. Osakabe,
Measurement of Neutron Energy on D-T Fusion Plasma Experiments;
Apr. 1995

NIFS-348 M. Sita Janaki, M.R. Gupta and Brahmananda Dasgupta,
Adiabatic Electron Acceleration in a Cnoidal Wave; Apr. 1995

NIFS-349 J. Xu, K. Ida and J. Fujita,
A Note for Pitch Angle Measurement of Magnetic Field in a Toroidal Plasma Using Motional Stark Effect; Apr. 1995

NIFS-350 J. Uramoto,
Characteristics for Metal Plate Penetration of a Low Energy Negative Muonlike or Pionlike Particle Beam: Apr. 1995

NIFS-351 J. Uramoto,
An Estimation of Life Time for A Low Energy Negative Pionlike Particle Beam: Apr. 1995

NIFS-352 A. Taniike,
Energy Loss Mechanism of a Gold Ion Beam on a Tandem Acceleration System: May 1995

NIFS-353 A. Nishizawa, Y. Hamada, Y. Kawasumi and H. Iguchi,
Increase of Lifetime of Thallium Zeolite Ion Source for Single-Ended Accelerator: May 1995

NIFS-354 S. Murakami, N. Nakajima, S. Okamura and M. Okamoto,
Orbital Aspects of Reachable β Value in NBI Heated Heliotron/Torsatrons; May 1995

NIFS-355 H. Sugama and W. Horton,
Neoclassical and Anomalous Transport in Axisymmetric Toroidal Plasmas with Electrostatic Turbulence; May 1995

NIFS-356 N. Ohyabu
A New Boundary Control Scheme for Simultaneous Achievement of H-mode and Radiative Cooling (SHC Boundary); May 1995

NIFS-357 Y. Hamada, K.N. Sato, H. Sakakita, A. Nishizawa, Y. Kawasumi, R. Liang, K. Kawahata, A. Ejiri, K. Toi, K. Narihara, K. Sato, T. Seki, H. Iguchi, A. Fujisawa, K. Adachi, S. Hidekuma, S. Hirokura, K. Ida, M. Kojima, J. Koong, R. Kumazawa, H. Kuramoto, T. Minami,. M. Sasao, T. Tsuzuki, J.Xu, I. Yamada, and T. Watari,
Large Potential Change Induced by Pellet Injection in JIPP T-IIU Tokamak Plasmas; May 1995

NIFS-358	M. Ida and T. Yabe, *Implicit CIP (Cubic-Interpolated Propagation) Method in One Dimension*; May 1995
NIFS-359	A. Kageyama, T. Sato and The Complexity Simulation Group, *Computer Has Solved A Historical Puzzle: Generation of Earth's Dipole Field*; June 1995
NIFS-360	K. Itoh, S.-I. Itoh, M. Yagi and A. Fukuyama, *Dynamic Structure in Self-Sustained Turbulence*; June 1995
NIFS-361	K. Kamada, H. Kinoshita and H. Takahashi, *Anomalous Heat Evolution of Deuteron Implanted Al on Electron Bombardment*; June 1995
NIFS-362	V.D. Pustovitov, *Suppression of Pfirsch-schlüter Current by Vertical Magnetic Field in Stellarators*; June 1995
NIFS-363	A. Ida, H. Sanuki and J. Todoroki *An Extended K-dV Equation for Nonlinear Magnetosonic Wave in a Multi-Ion Plasma*; June 1995
NIFS-364	H. Sugama and W. Horton *Entropy Production and Onsager Symmetry in Neoclassical Transport Processes of Toroidal Plasmas;* July 1995
NIFS-365	K. Itoh, S.-I. Itoh, A. Fukuyama and M. Yagi, *On the Minimum Circulating Power of Steady State Tokamaks*; July 1995
NIFS-366	K. Itoh and Sanae-I. Itoh, *The Role of Electric Field in Confinement*; July 1995
NIFS-367	F. Xiao and T. Yabe *A Rational Function Based Scheme for Solving Advection Equation;* July 1995
NIFS-368	Y. Takeiri, O. Kaneko, Y. Oka, K. Tsumori, E. Asano, R. Akiyama, T. Kawamoto and T. Kuroda, *Multi-Beamlet Focusing of Intense Negative Ion Beams by Aperture Displacement Technique;* Aug. 1995
NIFS-369	A. Ando, Y. Takeiri, O. Kaneko, Y. Oka, K. Tsumori, E. Asano, T. Kawamoto, R. Akiyama and T. Kuroda, *Experiments of an Intense H- Ion Beam Acceleration*; Aug. 1995